THE JOURNAL OF BIOLOGICAL CHEMISTRY VOL. 284, NO. 24, pp. 16584–16594, June 12, 2009
Printed in the U.S.A.

Molecular and Functional Analyses of Amino Acid Decarboxylases Involved in Cuticle Tanning in *Tribolium castaneum*[*] [S]

Received for publication, March 11, 2009 Published, JBC Papers in Press, April 14, 2009, DOI 10.1074/jbc.M901629200

Yasuyuki Arakane[‡], Joseph Lomakin[§], Richard W. Beeman[¶], Subbaratnam Muthukrishnan[‡], Stevin H. Gehrke[§], Michael R. Kanost[‡1], and Karl J. Kramer[‡¶]

From the [‡]Department of Biochemistry, Kansas State University, Manhattan, Kansas 66506, the [§]Department of Chemical and Petroleum Engineering, University of Kansas, Lawrence, Kansas 66045, and the [¶]Grain Marketing and Production Research Center, Agricultural Research Service-United States Department of Agriculture, Manhattan, Kansas 66502

Aspartate 1-decarboxylase (ADC) and 3,4-dihydroxyphenylalanine decarboxylase (DDC) provide β-alanine and dopamine used in insect cuticle tanning. β-Alanine is conjugated with dopamine to yield *N*-β-alanyldopamine (NBAD), a substrate for the phenol oxidase laccase that catalyzes the synthesis of cuticle protein cross-linking agents and pigment precursors. We identified ADC and DDC genes in the red flour beetle, *Tribolium castaneum* (*Tc*), and investigated their functions. *TcADC* mRNA was most abundant prior to the pupal-adult molt. Injection of *TcADC* double-stranded (ds) RNA (ds*TcADC*) into mature larvae resulted in depletion of NBAD in pharate adults, accumulation of dopamine, and abnormally dark pigmentation of the adult cuticle. Injection of β-alanine, the expected product of ADC, into ds*TcADC*-treated pupae rescued the pigmentation phenotype, resulting in normal rust-red color. A similar pattern of catechol content consisting of elevated dopamine and depressed NBAD was observed in the genetic *black* mutants of *Tribolium*, in which levels of *TcADC* mRNA were drastically reduced. Furthermore, from the *Tribolium black* mutant and ds*TcADC*-injected insects both exhibited similar changes in material properties. Dynamic mechanical analysis of elytral cuticle from beetles with depleted *TcADC* transcripts revealed diminished cross-linking of cuticular components, further confirming the important role of oxidation products of NBAD as cross-linking agents during cuticle tanning. Injection of ds*TcDDC* into larvae produced a lethal pupal phenotype, and the resulting grayish pupal cuticle exhibited many small patches of black pigmentation. When ds*TcDDC* was injected into young pupae, the resulting adults had abnormally dark brown body color, but there was little mortality. Injection of ds*TcDDC* resulted in more than a 5-fold increase in levels of DOPA, indicating that lack of TcDDC led to accumulation of its substrate, DOPA.

Insect cuticle tanning (sclerotization and pigmentation) is a complex process that involves the oxidative conjugation and cross-linking of cuticular proteins by quinones, which renders the proteins insoluble and also hardens and darkens the exoskeleton (1). The quinones are derived from catecholic metabolites of the amino acid tyrosine, produced by a series of enzymatic modifications, including hydroxylation, decarboxylation, *N*-acyl transfer, and oxidation (Fig. 1) (2). During tanning, cross-links form between adjacent polypeptide chains, causing progressive hardening, dehydration, and close packing of the polymers. This cross-linking occurs as a result of reactions of quinones and quinone methides derived from *N*-acylcatecholamines with nucleophilic side chain groups of structural proteins, leading to changes in mechanical properties and coloration (3). The major catechols used by insects as cuticle tanning agent precursors are dopamine, *N*-β-alanyldopamine (NBAD),[2] and *N*-acetyldopamine (NADA) (1).

Different types of quinones and quinone methides produced from catecholic metabolites may contribute to the variety of physical properties of insect cuticle. For example, NADA is predominant in the unpigmented hard larval head capsule of *Manduca sexta* (tobacco hornworm), whereas the hard pigmented cuticles of the larval mandible and pupa contain primarily NBAD (4, 5). However, both NADA and NBAD are major catechols in the rust-red colored cuticle of the red flour beetle, *Tribolium castaneum* (6, 7). Previously, we analyzed the levels of catechols and β-alanine in both wild-type (rust-red body color) and black body color mutant strains of *Tribolium*, and we demonstrated that the *black* mutant had decreased concentrations of β-alanine and NBAD when compared with levels present in wild-type beetles (6). The *black* mutation influenced not only cuticle pigmentation but also the puncture resistance of the cuticle, suggesting that both β-alanine and NBAD are critical for beetle cuticle tanning (7). The precise genetic basis for the black and other dark body mutations, however, was not established.

* This work was supported by National Science Foundation Grant IOS 0726425. This is Contribution 08-298-J from the Kansas Agricultural Experiment Station.

[S] The on-line version of this article (available at http://www.jbc.org) contains supplemental Figs. S1 and S2.

The nucleotide sequence(s) reported in this paper has been submitted to the GenBank™/EBI Data Bank with accession number(s) EU019709, EU019710, and EU302526.

[1] To whom correspondence should be addressed: Dept. of Biochemistry, 141 Chalmers Hall, Kansas State University, Manhattan, KS 66506. Tel.: 785-532-6121; Fax: 785-532-7278; E-mail: kanost@ksu.edu.

[2] The abbreviations used are: NBAD, *N*-β-alanyldopamine; DOPA, 3,4-dihydroxyphenylalanine; NADA, *N*-acetyldopamine; AMD, α-methyldopa; DA, dopamine; DMA, dynamic mechanical analysis; RNAi, RNA interference; RT, reverse transcription; dsRNA, double-stranded RNA; TcADC, *T. castaneum* aspartate 1-decarboxylase; TcDDC, *T. castaneum* DOPA decarboxylase; dsRNA, double-stranded RNA; HPLC, high pressure liquid chromatography.

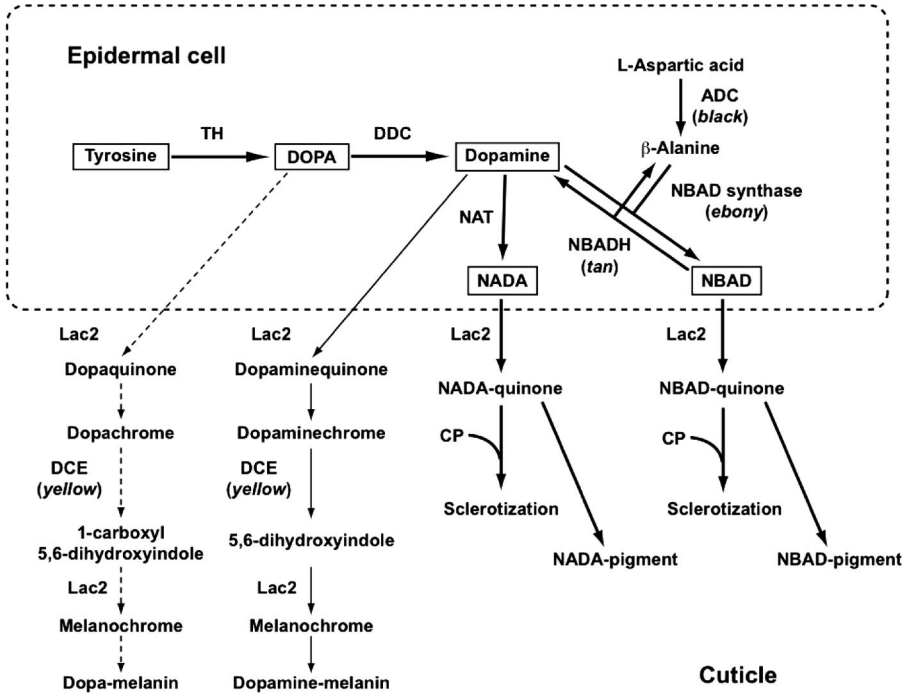

FIGURE 1. **Proposed cuticle pigmentation and sclerotization metabolic pathway in *T. castaneum*.** *TH,* tyrosine hydroxylase; *DOPA,* 3,4-dihydroxyphenylalanine; *Dopamine*, 3,4-dihydroxyphenethylamine; *Ebony,* *N*-β-alanyldopamine synthase; *NBADH,* *N*-β-alanyldopamine hydrolase; *DCE*, dopachrome conversion enzyme; *Lac2*, laccase 2; *CP,* cuticle protein(s). The *solid* and *dotted lines* represent proposed major and minor reactions for cuticle tanning in *Tribolium*.

Two related decarboxylases, aspartate 1-decarboxylase (ADC, EC 4.1.1.11) and DOPA decarboxylase (DDC, EC 4.1.1.28), are predicted to be involved in the *Tribolium* cuticle sclerotization and pigmentation pathway, and each is a candidate for the gene that is mutated in *black*. ADC catalyzes the synthesis of β-alanine by decarboxylation of the α-COOH group of L-aspartic acid. β-Alanine subsequently plays a critical role in cuticle tanning because of its conjugation with dopamine to produce NBAD (6, 8–10). DDC catalyzes the conversion of DOPA to dopamine. To examine more fully the functional roles of ADC and DDC in the synthesis of catechols in the *Tribolium* cuticle tanning pathway, and to determine whether those enzymes and their products influence the physical properties of the cuticle, we performed RNA interference (RNAi) experiments to suppress the transcript levels of the corresponding genes. The levels of catechols in insects subjected to RNAi and in wild-type insects and the two mutants, *black* and b^{Chr}/b^{ST}, were analyzed by HPLC with electrochemical detection. These experiments were then followed by measurement of the dynamic mechanical properties of the elytra to determine the effects of altered catechol and β-alanine content on physical properties of the exoskeleton. Such tests can distinguish between cross-linked and uncross-linked high molecular weight compounds, a distinction key to evaluating the roles of enzymes and metabolites in cuticle tanning.

EXPERIMENTAL PROCEDURES

Chemicals—3,4-Dihydroxyphenylalanine (DOPA), 3,4-dihydroxyphenylethylamine (dopamine, DA), the internal standard, 2-methyl-3-(3,4-dihydroxyphenyl)alanine (α-methyldopa, AMD), and *N*-acetyldopamine (NADA) were purchased from Sigma. *N*-β-Alanyldopamine (NBAD) was obtained from the Chemical Synthesis and Drug Supply Program of NIMH (nimh-repository.rti.org). All reagents were of the highest purity available. Other chemicals, unless noted otherwise, were purchased from Fisher.

Insects—*T. castaneum* (Coleoptera, Tenebrionidae) strain GA-1 (11) and two black body color mutants, *black* and b^{Chr}/b^{ST}, were reared at 30 °C under standard conditions (12). The *black* mutation is a spontaneous, incompletely recessive, homozygous viable mutation on the third chromosomal linkage group (13). The *Charcoal* (b^{Chr}) and *black-of-Scott-Thomson* (b^{ST}) mutations are radiation-induced, dominant, homozygous lethal alleles of *black* (14). The lethality of each of the latter two alleles appears to be due to an independent lesion in an unrelated gene pseudolinked by chromosome rearrangement to a nonlethal lesion in the *black* gene. Thus, b^{Chr}/b^{ST} forms a balanced lethal system.

Cloning of the T. castaneum Aspartate 1-Decarboxylase (TcADC) and DOPA Decarboxylase (TcDDC) cDNAs—Putative amino acid decarboxylase genes in *Tribolium*, including *TcADC* and *TcDDC*, were identified by searching Beetlebase using *Drosophila* Dgad2 (CG7811-RA) and the DOPA decarboxylase, epidermal form (CG10697-RB, 15) as queries, respectively. To clone the partial cDNAs of *TcADC* and *TcDDC*, the following primers were used: 5′-AGG GAA CGA ACC GCA AGA AC-3′ and 5′-CAA GGC CTT AAA GAT CGC TC-3′ for *TcADC*, and 5′-GGT GAA TTG ACT CTA GTG TTT AG-3′ and 5′-CGT AAC TTA AGT CTA GAT TGT CTT C-3′ for *TcDDC*. 5′- and 3′-rapid amplifications of cDNA ends (Invitrogen) were performed to obtain the full-length cDNA of *TcADC*. The sequences of *TcADC* and *TcDDC* cDNAs have been deposited in GenBank™ with the accession numbers EU019709 and EU019710, respectively. The sequence of *TcADC* from the *black* body color mutant was also deposited in GenBank™ with the accession number EU302526.

Gene Expression Analysis by RT-PCR and Real Time PCR—To analyze expression profiles of *TcADC* and *TcDDC* genes, total RNA was isolated from whole insects at the pharate pupal to adult stages by using the RNeasy mini kit (Qiagen). cDNA synthesis and RT-PCR were done as described previously (16) using the primer pair 5′-ACA ACG TCT ACT TGA TAC G-3′ and 5′-GTC GTA TTT GGT GTC GTA G-3′ for *TcADC*, and the primer pair 5′-ATG GAA GCT AAT CAG TTC AAG G-3′ and 5′-TCC AGC ATC ACG ACT TCT AG-3′ for *TcDDC*. As an internal control, the following pair of primers designed for *Tribolium* ribosomal protein S6 (rpS6) were used: 5′-AGA TAT ATG GAA GCA TCA TGA AGC-3′ and 5′-CGT CGT

CTT CTT TGC TCA AAT TG-3′. To analyze the transcript levels of *TcADC* in the three strains, GA-1 (wild type), *black*, and b^{Chr}/b^{ST}, total RNAs were isolated from whole insects 5–6 days after pupation (pharate adults). Real time PCR was performed using SYBR Premix Ex Taq (Takara) and the Mx3000PTM real time PCR System (Stratagene). The following pairs of primers were used: 5′-TGC CAG ATA CAG GTT TAT GCC CGA-3′ and 5′-GAT GCC TTG GAA AGA GGC GAG TTT-3′ for *TcADC*; 5′-CGT GAG GCT GGC CTT ATT CCA TTT-3′ and 5′-GTG CAG CCA GAT GTT GTT CGA GTT-3′ for *TcDDC*; and 5′-ACG CAA GTC AGT TAG AGG GTG CAT-3′ and 5′-TCC TGT TCG CCT TTA CGC ACG ATA-3′ for *TcrpS6* as an internal control. To analyze the knockdown level of *TcADC* transcripts, dsRNA for *TcADC* was injected into penultimate- or last-instar larvae, and total RNA was isolated 5–6 days after pupation (13–14 days post-injection).

Synthesis of dsRNAs and Injection into Insects— dsRNAs for *TcADC*, *TcDDC*, and *T. castaneum vermilion* (*Tcv*) (17) were prepared according to the protocol described previously using the AmpliScribe T7-Flash transcription kit (Epicenter Technologies) (18). ds*Tcv* was used as a negative control dsRNA in this study. The *vermilion* gene (*v*) encodes tryptophan oxygenase (EC 1.13.1.11) that catalyzes the conversion of tryptophan to *N*-formylkynurenine in the ommochrome pigment pathway and is required for dark eye pigmentation in *Tribolium* and other insects, but it lacks any apparent role in cuticle formation (19). The length of the dsRNAs for *TcADC*, *TcDDC*, and *Tcv* were 433 bp (nucleotides 1192–1624), 301 bp (nucleotides 1251–1551), and 609 bp (nucleotides 310–918), respectively. dsRNAs for laccase 2 (*TcLac2*) and tyrosinase (*TcTyr*) were prepared as described by Arakane *et al.* (19). For RNAi experiments, 200 ng of the dsRNA were injected into penultimate- and/or last-instar larvae of strains GA-1 (wild type), *black*, and b^{Chr}/b^{ST} (20). After injection, larvae were kept at 30 °C for visual monitoring of phenotypes and other analyses.

Phylogenetic Analysis of Decarboxylases—A core region of homologous sequence highly conserved in all decarboxylases, including a putative catalytic region, was aligned with ClustalW software prior to phylogenetic analysis. The MEGA 3.0 program (21) was used to construct the consensus phylogenetic tree using the Unweighted Pair Group Method with Arithmetic Mean. To evaluate the branch strength of the phylogenetic tree, bootstrap analysis of 5,000 replications was performed.

Extraction of Catechols—To analyze the levels of catechols such as DOPA, dopamine, NADA, and NBAD, three groups of five pharate adults each were weighed and homogenized in a glass tissue grinder in 0.5 ml of ice-cold 0.1 M perchloric acid containing 1 mM EDTA and 1 mM sodium metabisulfite to minimize oxidation of the catechols. The extracts were subsequently centrifuged at 13,000 × *g* for 30 min at 4 °C, and the supernatants were used for the analyses.

Catechol Analysis—Extracts were resolved and analyzed using an HP 1050 HPLC system fitted with a programmable HP 1049A electrochemical detector. Twenty μl of each sample was loaded onto a C18 reversed phase column (Gemini, 250 × 4.6 mm, 5 μm) obtained from Phenomenex (Torrance, CA) using an HP autosampler and a sequence program. Catechols were resolved using an isocratic mobile phase consisting of 12% acetonitrile containing 1.4 mM octane sulfonic acid as an ion-pairing agent, 1 mM EDTA, and 1 mM lithium chloride, pH 3.05, at a flow rate of 0.5 ml/min. The catechols were detected using the electrochemical detector with a glassy carbon electrode and the oxidative potential set at +700 mV. DA, DOPA, NADA, AMD, and NBAD were identified by their retention times in comparison with the known standards as follows: DOPA, 6.8; NADA, 11.1; AMD, 11.9; DA, 12.9; and NBAD, 23.5 min. All samples were run in two replicates. The detection limit was ≤0.1 μM, and the recovery was ≥95%. Quantitation was accomplished by comparing peak areas of beetle catechols with those of the corresponding standards of known concentrations and using AMD as an internal standard. Peak areas and retention times were computed using a PC aided by HP ChemStation version revised 08.03 software.

Mechanical Testing of Elytra from Tribolium—At 7–14 days after ecdysis, adult beetles were sacrificed by exposure to −20 °C for 30 min, and then elytra were immediately removed with forceps and mounted onto a custom sample holder with Devcon 1.5-Ton quick-setting epoxy cement. The fast-setting epoxy was allowed to dry for 1 h prior to testing, fixing the samples in place without damage. Sample dimensions were determined via calipers and microscopic measurements using a digital micrometer. A TA Instruments RSAIII dynamic mechanical analyzer was used to perform all of the dynamic mechanical measurements under ambient conditions. The instrument was used to apply a sinusoidally oscillating tension stress on an elytron and to record the strain response. The lag between stress and strain is a function of the elastic (cross-linked) *versus* the viscous (noncross-linked) response of a sample.

Strain sweeps at 1 Hz (measuring stress as strain amplitude is gradually increased at constant frequency) were used to determine the extent of the linear viscoelastic region of the elytron, the region where an applied strain maintains a linear stress-strain response and where the processes are reversible. This is a necessary prerequisite to frequency sweep tests, as it ensures that the results are strain-independent and that the applied force does not damage a sample during the course of the experiment (22). For all of the elytral types tested, the material properties were found to be strain-independent beyond a strain of 0.2%, and instrument noise was acceptable at this value. Thus, a strain of 0.2% was used for all of the reported frequency sweep experiments.

RESULTS

Characterization of TcADC and TcDDC Genes and Encoded Proteins—Searching Beetlebase with the tblastn program using the sequences of two *Drosophila* enzymes, Dgad2 (= black, an aspartate decarboxylase) and DOPA decarboxylase (epidermal form), revealed 11 *Tribolium* genes that encode members of the pyridoxal phosphate-dependent amino acid decarboxylase family, in which all members exhibit a large and highly conserved pyridoxal-dependent decarboxylase domain with a pyridoxal phosphate-binding motif, Ser-*X*-*X*-Lys (Fig. 2 and supplemental Fig. 1). In comparison, the *Drosophila melanogaster*

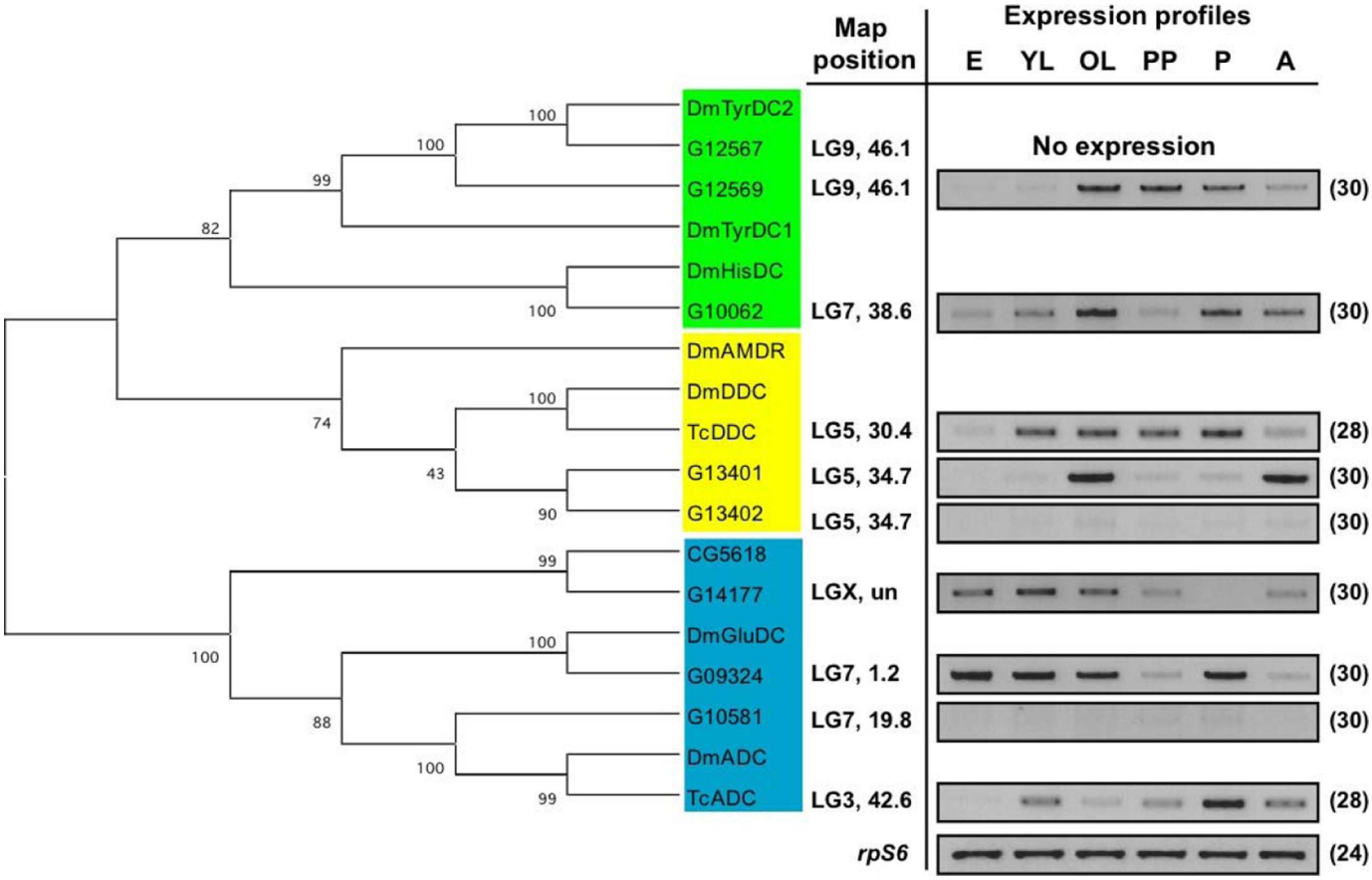

FIGURE 2. **Phylogenetic analysis of amino acid decarboxylases in *Tribolium* and *Drosophila*.** The phylogenetic tree was constructed by MEGA 3.0 software using Unweighted Pair Group Method with Arithmetic Mean. *Numbers* by each branch indicate results of bootstrap analysis of 5,000 replications. See supplemental Fig. 1 for the accession numbers of protein sequences used here. For the expression profiles of amino acid decarboxylases in *Tribolium* by RT-PCR, total RNA was extracted from whole beetles ($n = 5$) at various developmental stages from embryos to adult. *E,* embryos; *YL,* young larvae; *OL,* old larvae; *PP,* pharate pupae; *P,* pupae; *A,* adults. The *numbers* in *parentheses* represent PCR cycles. *un,* unknown.

genome contains only nine members of this gene family. The encoded proteins can be divided into three major clades as follows: with clade A (*green* in Fig. 2), including *Drosophila* histidine and tyrosine decarboxylases; clade B (*yellow* in Fig. 2), including *Drosophila* DOPA decarboxylase (DmDDC) and the α-methyl DOPA resistance gene (DmAMDR); and the more distantly related clade C (*blue* in Fig. 2) containing the *Drosophila* aspartate decarboxylase (DmADC) and glutamate decarboxylase (DmGluDC) proteins. Another *D. melanogaster* gene, *CG1486*, and a highly related *T. castaneum* gene, *G05445*, encode several long insertions in the conserved domain. The latter two genes were not included in this phylogenetic analysis, but they would define a fourth, more distant clade (data not shown). Putative *T. castaneum* orthologs can be identified for *Drosophila* Tyr decarboxylase 2 (G12567), His decarboxylase (G10062), DDC (G13480), GluDC (G09324), and ADC or black (G00038). However, additional *T. castaneum* genes are represented in the branches that contain TyrDC, DDC, and ADC, indicating that expansions of this gene family have occurred in the red flour beetle. For this study, we have further analyzed the *Tribolium* genes that are most closely related to *DmDDC* and *DmADC*.

We cloned and sequenced multiple full-length cDNAs encoding TcADC from the wild-type GA-1 strain and the black body color mutant to analyze whether any mutations could be detected in the transcript from *black* individuals. The GA-1 *TcADC* cDNA sequence was identical to the transcript predicted from the genome except for one nucleotide that did not result in an amino acid substitution. However, it differed from the *TcADC* cDNA prepared from the *black* strain at 14 nucleotide positions, which resulted in only four conservative amino acid substitutions (supplemental Fig. 2). However, none of these mutations resulted in an amino acid substitution in the putative decarboxylase catalytic domain, and none created a premature stop codon in the open reading frame. As the wild-type and black body color strains are not closely related, the minor sequence differences in the *TcADC* transcripts may be due to allelic variation that would not be expected to significantly affect enzyme function. Therefore, the black phenotype is unlikely to be due to production of a nonfunctional ADC. Instead, results presented below demonstrate that *TcADC* transcript levels are much lower in the *black* mutants than in the wild-type beetles.

We also cloned and sequenced a cDNA encoding TcDDC from the GA-1 strain and found the sequence to be identical to the transcript predicted from the genome, except for seven nucleotide differences that resulted in only one amino acid substitution (Met to Lys at position 450). The amino acid sequence identities of TcADC and TcDDC with other insect ADC-like

TABLE 1

Amino acid identity/(similarity) of insect ADCs

T. castaneum, TcADC; EU019709; *Anopheles gambiae*, AgADC: XP_319650; *A. aegypti*, AaADC; XP_001658435; *D. melanogaster*, DmADC (DGAD2): NP_476788; and *Apis mellifera*, AmADC: XP_39523.

	TcADC	DmADC	AgADC	AaADC	AmADC
TcADC		53.0	64.4	63.8	58.1
DmADC	(67.3)		56.6	57.3	53.7
AgADC	(75.5)	(68.8)		84.0	56.2
AaADC	(77.5)	(71.3)	(91.0)		57.3
AmADC	(74.8)	(68.6)	(70.0)	(71.3)	

TABLE 2

Amino acid identity/(similarity) of insect DDCs

T. castaneum, TcDDC: EU019710; *A. gambiae*, AgDDC: XP_319840; *A. aegypti*, AaDDC: XP_001648263: *D. melanogaster*, DmDDC: NP_724164; *A. mellifera*, AmDDC: XP_394115; *M. sexta*, MsDDC: AAC46604; *Bombyx mori*, BmDDC: NP_001037174; and *Tenebrio molitor*, TmDDC: BAA95568.

	TcDDC	DmDDC	AgDDC	AaDDC	MsDDC	BmDDC	TmDDC
TcDDC		73.7	74.8	72.5	68.7	75.3	91.8
DmDDC	86.1)		77.3	78.9	66.7	73.6	75.6
AgDDC	(86.7)	(88.3)		85.0	66.4	72.7	75.2
AaDDC	(85.0)	(89.1)	(92.0)		66.8	72.3	73.5
MsDDC	(80.9)	(77.1)	(77.7)	(78.1)		83.3	69.7
BmDDC	(87.7)	(84.7)	(85.2)	(85.9)	(88.6)		75.5
TmDDC	(96.4)	(87.4)	(85.5)	(84.6)	(80.1)	(86.8)	

and DDC-like proteins range from 67 to 91% and 77 to 96%, respectively (Tables 1 and 2).

Expression Profiles of TcADC and TcDDC Genes—Developmental patterns of expression of ds*TcADC* and ds*TcDDC* were determined by RT-PCR and real time PCR using RNA prepared from eggs, larvae, pharate pupal, pupal, and adult stages (Figs. 2 and 3*A*). The highest levels of *TcADC* transcripts were detected in the pharate adult and the young adult just before and after the pupal to adult molt. Transcripts of *TcDDC* were observed at all stages, with much higher levels detected in the pharate adult. Of the two other genes that encode proteins quite similar in sequence to TcDDC and therefore expected to exhibit DDC activity, *G13401* is expressed at a low level in eggs and young larvae, and during the first 3 days of the pupal stage. However, transcript levels are much higher in older larvae and after the adult molt (Fig. 2 and Fig. 3*A*). *G13402*, on the other hand, exhibited little or no expression at any developmental stage.

Expression of *TcADC* and *TcDDC* in pharate adults from three different beetle strains, wild type, *black*, and b^{Chr}/b^{ST}, was analyzed by RT-PCR and real time RT-PCR (Fig. 3*B*). The level of *TcADC* transcripts in *black* was more than 2 orders of magnitude less than that found in the wild-type strain. An even greater difference from the wild type was observed in the b^{Chr}/b^{ST} *black* body color mutant strain, in which *TcADC* transcripts were undetectable. In contrast, no difference between the strains was detected in the levels of transcripts for *TcDDC* or the ribosomal protein S6 that was used as an internal control. These results indicate that *TcADC* is severely underexpressed in the two mutant strains that display the black phenotype. Experiments described below further examine whether a lack of *TcADC* expression might cause the black phenotype due to an insufficient supply of β-alanine.

Effect of Injection of Double-stranded RNA for TcADC on Cuticle Pigmentation and Catechol Levels—To examine the function of ADC *in vivo*, we injected dsRNA (200 ng per insect) for *TcADC* into penultimate- and last-instar larvae and observed the resulting phenotypes. The level of *TcADC* transcripts observed after injection of dsRNA for *TcADC* was less than 10% of that detected in controls, indicating that a substantial knockdown of *TcADC* expression had occurred (Fig. 4*B*). Insects injected with ds*TcADC* displayed darkened body pigmentation when compared with controls (Fig. 4*A*). Pupa-specific cuticular structures such as the gin traps were darker than those of control insects (data not shown). This effect, however, was most striking in adults, which were black rather than the rust-red color of uninjected beetles or controls injected with a different dsRNA. Wild-type adults treated with ds*TcADC* had the same body color as the *black* mutant strains.

Previously, we demonstrated that injection of β-alanine into the black body color mutant restored the rust-red pigmentation of the adult cuticle (6). We conducted a similar experiment to determine whether β-alanine injection could also rescue the black body color phenotype produced by injection of dsRNA for *TcADC,* restoring the normal rust-red pigmentation. As shown in Fig. 5, a successful rescue of black adult pigmentation was obtained after injection of β-alanine, the expected product of ADC, into ds*TcADC*-treated pharate adults.

Levels of catechols in ds*TcADC*-treated insects were compared with those in controls (ds*Tcv*-treated wild-type insects) and the two *black* mutant strains (Fig. 6). After *TcADC* knockdown NBAD content of pharate adults was decreased nearly 10-fold when compared with controls (Fig. 6*A*). The *black* mutant strains also had significantly lower NBAD content than wild-type controls as well as higher levels of dopamine (Fig. 6*B*). These data are consistent with the hypothesis that the black body color mutant has a defect(s) in the gene encoding ADC and that the black phenotype is a result of an abnormally low expression of ADC, which leads to a deficiency in β-alanine required for the synthesis of NBAD.

Effect of Injection of Double-stranded RNAs for Two Phenol Oxidases, TcLac2 and TcTyr, on Cuticle Pigmentation of the Black Mutant—We previously demonstrated that laccase 2 is responsible for cuticle tanning in wild-type *T. castaneum*, in which NADA, NBAD, and dopamine are the predominant catechols available as laccase substrates (19). To test whether either or both of the phenol oxidases, laccase and tyrosinase, catalyze cuticle tanning in the black body color mutant that has a reduced NBAD content, dsRNA (200 ng per insect) for *TcLac2* or the two *TcTyr* genes was injected into last-instar larvae or pharate pupae of the b^{Chr}/b^{ST} mutant. Tanning of cuticle was almost completely prevented by injection of ds*TcLac2*, whereas injection of either ds*TcTyr* had no effect (Fig. 7). These results are consistent with those reported from previous *TcLac2* and *TcTyrs* RNAi experiments using the wild-type strain GA-1 (19) and support the following hypotheses: 1) laccase and not tyrosinase catalyzes both sclerotization and pigmentation of *Tribolium* larval,

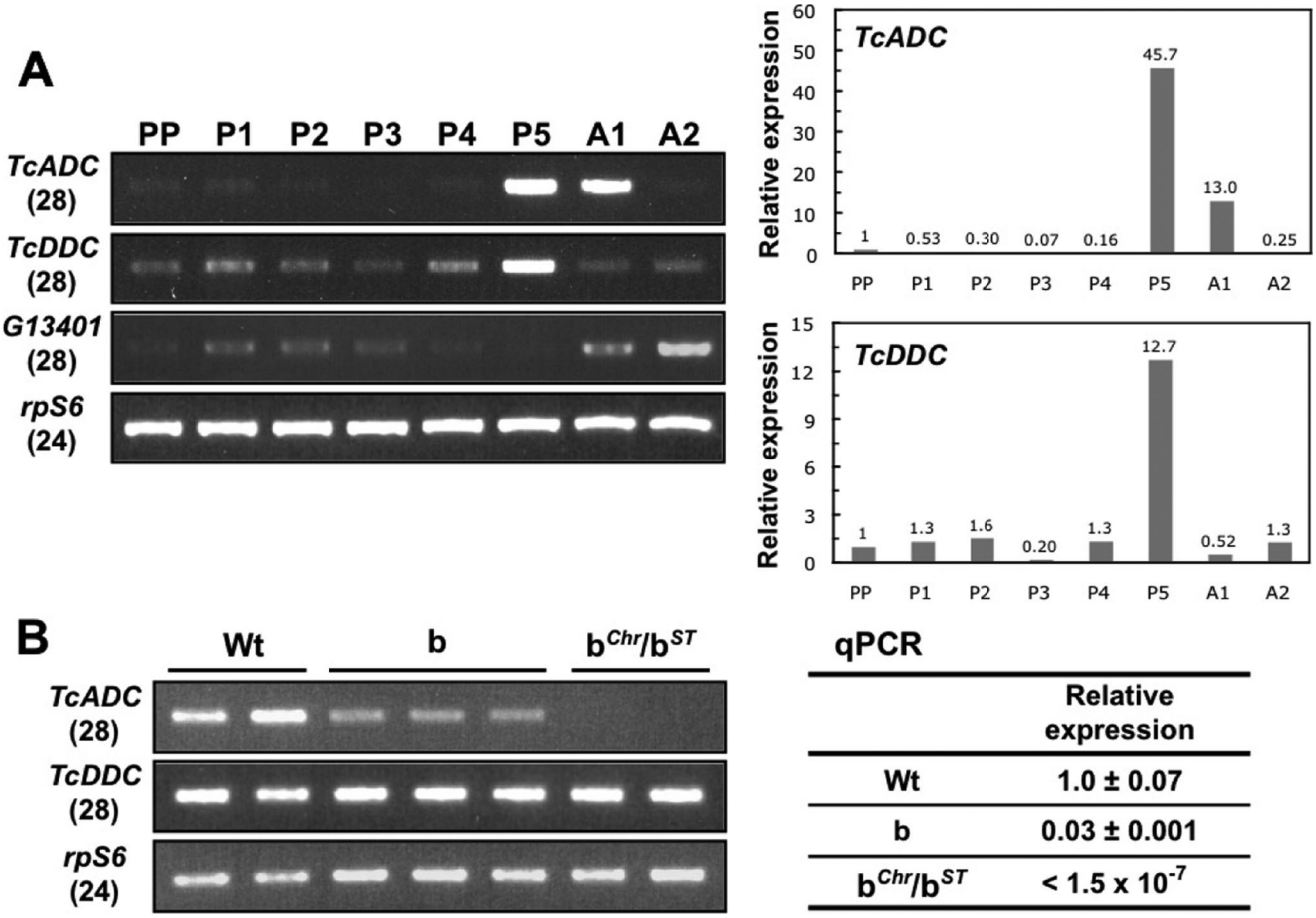

FIGURE 3. **Expression profiles of *TcADC* and *TcDDC* mRNAs during development.** *A*, total RNA was extracted from whole beetles ($n = 5$) at late developmental stages (pharate pupa to young adult). *PP*, pharate pupae; *P1*, 0–1-day-old pupae; *P2*, 1–2-day-old pupae, *P3*, 2–3-day-old pupae; *P4*, 3–4-day-old pupae; *P5*, 4–5-day-old pupae; *A1*, 0-day adults; *A2*, 5–6-day-old adults. *B*, expression levels of *TcADC* gene in the wild-type and two black body color mutants. cDNA templates for RT-PCR and real time PCR were prepared from total RNA isolated from whole beetles ($n = 5$, duplicate for wild-type and b^{Chr}/b^{ST}, and triplicate for Bl) at pharate adult stage corresponding to P5 in *A*. *Wt*, wild type; *b*, black body color mutant; b^{Chr}/b^{ST}, balanced lethal black body color mutant. The numbers in *parentheses* represent PCR cycles. RT-PCR and real time PCR of *Tribolium* ribosomal protein 6 (*rpS6*) transcript with the same cDNA template served as an internal control. For real time PCR, expression levels for *TcADC* and *TcDDC* are presented relative to the wild-type level or the levels of expression in pharate pupae (*PP*). *qPCR*, quantitative PCR.

pupal, and adult cuticles, and 2) black rather than rust-red pigmentation is due to an increased content of dopamine-quinone (and dopamine melanin) produced via oxidation of DA by laccase 2 along with a concomitant decrease in the NBAD quinone content.

Effect of Injection of Double-stranded RNA for TcDDC on Cuticle Pigmentation and Catechol Levels—As dopamine is required as a precursor for synthesis of NBAD and NADA, the predominant catechols utilized for cuticle tanning, we predicted that reduced TcDDC expression would result in aberrant sclerotization and pigmentation. We analyzed the function(s) of *TcDDC* by injection of dsRNA corresponding to a unique region of this gene. A lethal pupal phenotype was observed after injection of ds*TcDDC* into late larvae (Fig. 8). The resulting pupal cuticle attained a grayish color and exhibited many small black patches with a bilateral symmetry, after which all of the pupae died.

To evaluate the effect of down-regulation of *TcDDC* transcripts on adult cuticle tanning, ds*TcDDC* was injected into 1–2-day-old pupae. Pupae treated with ds*TcDDC* developed normally and molted to the adult stage, but tanning of the adult cuticle was delayed by several hours with the cuticle eventually becoming slightly darker than the normal rust-red color (Fig. 9). Levels of DOPA were more than 5-fold higher in ds*TcDDC*-treated insects (~1500 pmol/mg) relative to ds*Tcv*-treated control insects (~200 pmol/mg). However, an unexpected result was that injection of ds*TcDDC* did not result in any decrease in the levels of dopamine, NBAD, or NADA (data not shown).

Effect of Reduced TcADC Expression on Mechanical Properties of Elytral Cuticle—The tanning process involves not only pigment formation but also reactions of oxidized catechols that modify or cross-link cuticular proteins, modulating cuticular physical properties such as the elastic modulus, a measure of material stiffness. We used dynamic mechanical analysis (DMA) to test whether an altered catechol content resulting from reduced TcADC transcripts affects the physical properties of the cuticle in elytra from ds*TcADC*-treated beetles and black mutant beetles when compared with ds*Tcv*-injected control insects. DMA provides insight into the internal molecular structure of a material, in addition to direct measurement of fundamental material mechanical proper-

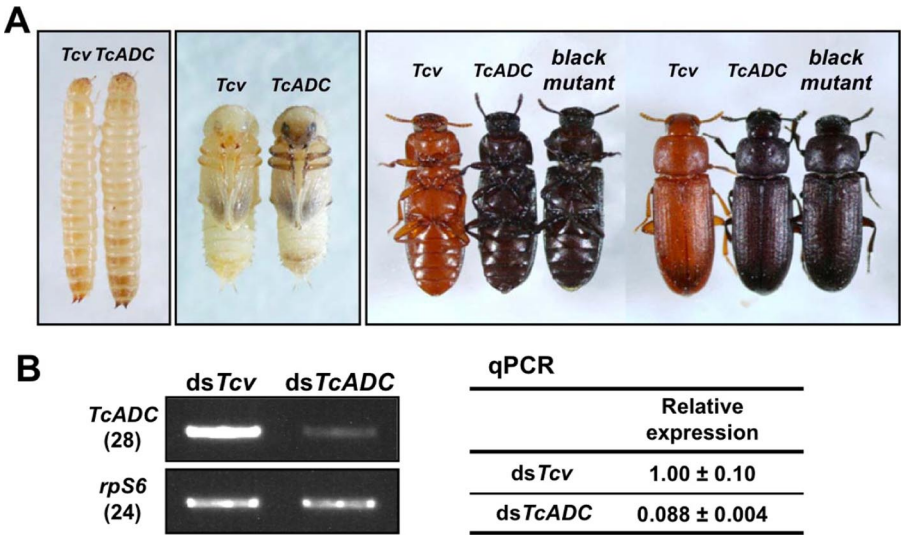

FIGURE 4. **Effect of dsRNA for *TcADC* on larval, pupal, and adult cuticle tanning.** *A,* dsRNA (200 ng per insect) for *TcADC* (ds*TcADC*) or *Tcv* (ds*Tcv*) were injected into penultimate instar or last instar larvae ($n = 60$, triplicate of 20 insects each). *Left panel,* 1-day-old last instar larvae; *middle panel,* 5-day-old pupae (pharate adults); *right panel,* 4-day-old adults. *B,* knockdown level of *TcADC* by RNAi. cDNAs for RT-PCR and real time PCR were prepared from total RNA isolated from whole beetles ($n = 3$) at 5 days (10-day post-injection). The *numbers* in *parentheses* represent PCR cycles. RT-PCR and real time PCR of *Tribolium* ribosomal protein 6 (*rpS6*) transcript with the same cDNA template served as an internal control. For real time PCR, expression levels of *TcADC* in ds*TcADC*-treated insects are presented relative to the levels in ds*Tcv* control. *qPCR,* quantitative PCR.

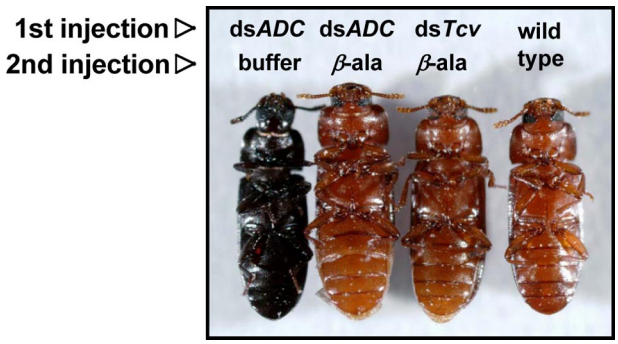

FIGURE 5. **Effect of injection of β-alanine on adult cuticle pigmentation of dsTcADC-treated *Tribolium* pupae.** dsRNAs for *TcADC* (ds*ADC*) *or Tcver* (ds*Tcv*) (200 ng per insect) were injected into 1-day-old pupae (1st injection), and then β-alanine (0.4 μmol per insect) or buffer were injected into 5-day-old pupae (2nd injection) ($n = 40$ for each treatment, duplicate of 20 insects each). Rescue of the black body adult phenotype produced by injection of ds*ADC* was observed by injection of β-alanine in 100% of the resulting adults.

ties, unlike more conventional mechanical measurements such as puncture resistance tests. Furthermore, because DMA does not require a material to be tested to failure, irreproducibility in sample preparation, mounting, and testing are minimized.

We performed frequency sweep experiments on tanned elytra freshly harvested prior to each test. Frequency sweep experiments on an elytron yield its complex modulus as function of the imposed oscillation stress frequency (ω). The complex modulus can be resolved into the elastic modulus (designated E′) and the viscous modulus (designated E″). The dependence of such moduli on frequency for polymeric materials in general is a function of the relaxation modes available to the constitutive polymer chains (23). The elastic modulus (E′) for an entangled, but uncross-linked, polymeric material is expected to increase with frequency, whereas E′ is expected to become frequency-independent for a well cross-linked material at frequencies below ~100 Hz (24, 25). Experimentally, the elastic modulus of a lightly cross-linked biopolymer is typically observed to have a weak power-law frequency dependence $E'(\omega) \sim \omega^{0.1\sim0.3}$. As the extent of cross-linking increases, the frequency exponent falls toward zero, exhibiting frequency independence (26, 27).

The E′ frequency dependence of the ds*TcADC* knockdown sample and the *black* mutant are remarkably similar to each other and significantly different from the control wild-type insects injected with ds*Tcv* (Fig. 10 and Table 3). An important, statistically confirmed similarity of the former two samples is indicated by the power law exponent (Table 3). Significantly, these exponents are more than 50% higher for the *black* and ds*TcADC*-treated elytra relative to that of the ds*Tcv*-injected control elytra. As noted earlier, the significantly higher E′ power law dependence of cuticle with reduced ADC levels suggests that the *black* and ds*TcADC* knockdown elytra are similar in having a less effectively cross-linked structure than ds*Tcv*-injected control elytra. This interpretation of the differences between the cuticle sets at the molecular level is further corroborated by the frequency dependence of the E″/E′ ratio (Fig. 11). The ratio of the E″ and the E′ (equivalent to *tan* δ, where δ is the phase angle between the applied stress and the material strain) has an inverse dependence on frequency, because viscous effects become relatively more important at low frequencies. Entangled, but uncross-linked, polymer chains are able to flow past one another at these longer time scales. Therefore, the ratio of E″/E′ is a function of the molecular interconnectivity, whether entangled or cross-linked. Uncross-linked materials exhibit relatively high viscous dampening and hence a high E″/E′ ratio. Cross-linking reduces the magnitude of the E″/E′ ratio as well as its inverse dependence on frequency (23). Elytra from the ds*ADC* knockdown insects and the black color mutant had a greater E″/E′ ratio and stronger inverse frequency dependence than elytra from the ds*Tcv* knockdown insects. This behavior demonstrates a higher dampening ability or viscous energy dissipation in elytra from ADC-deficient insects, consistent with the interpretation suggested by the data in Fig. 10 that the ADC-deficient insects have less effectively cross-linked cuticle than ds*Tcv*-injected insects. Overall, these data are consistent with the hypothesis that a product of *TcADC* mediates cross-linking and that the *black* mutant is deficient in ADC.

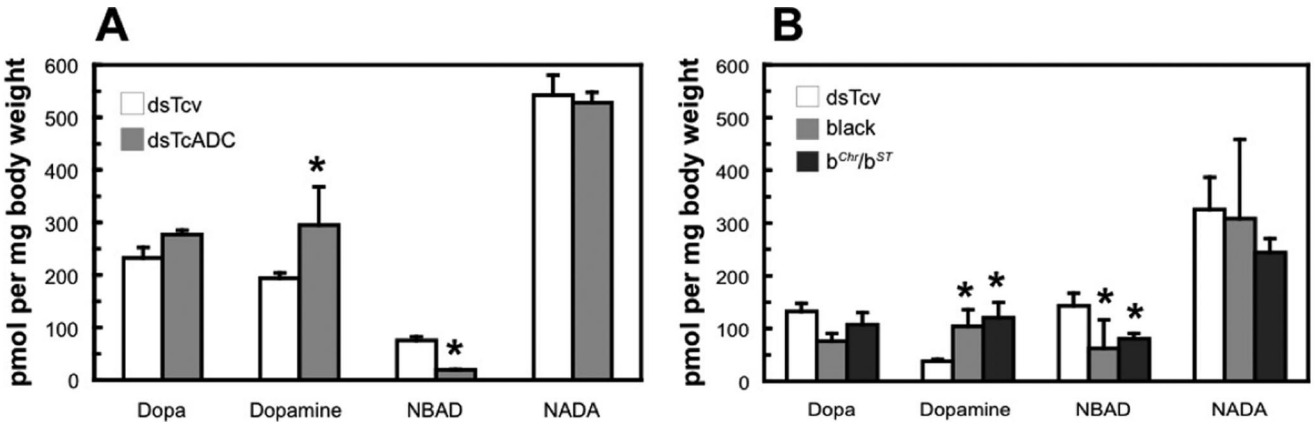

FIGURE 6. **Catechol content of *T. castaneum* pharate adults.** GA-1 wild-type larvae or pupae were injected with dsRNA for *TcADC* or *Tcv* (tryptophan oxygenase) as a control. When these insects became pharate adults, catechols were extracted and analyzed by HPLC with electrochemical detection (*A*). Catechols of untreated prepupae from two black body color mutants (*black* and b^{Chr}/b^{ST}) were also analyzed (*B*). *Bars* indicate mean ± S.D. ($n = 3$). Values significantly different from the ds*Tcv* controls ($p < 0.05$) are marked with an *asterisk* (determined by analysis of variance and Newman-Keuls multiple comparison test).

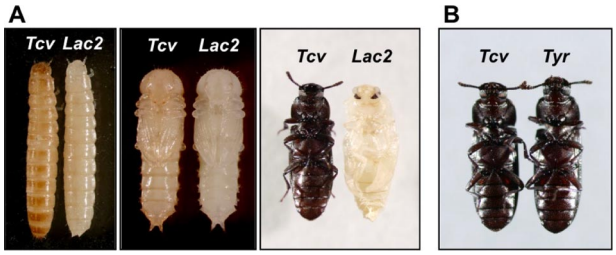

FIGURE 7. **Effect of dsRNA for *TcLac2* or *TcTyr* on larval, pupal, and adult cuticle tanning of b^{Chr}/b^{ST} black body color mutant.** dsRNA (200 ng per insect) for *TcLac2* or *TcTyr* was injected into late larvae or pharate pupae of b^{Chr}/b^{ST} black body color strain. Little or no cuticle tanning was observed after injection of ds*Lac2* at each developmental stage (*A*), whereas ds*Tyr* had no effect on cuticle tanning (*B*). dsRNA for *Tcv* was injected as a control.

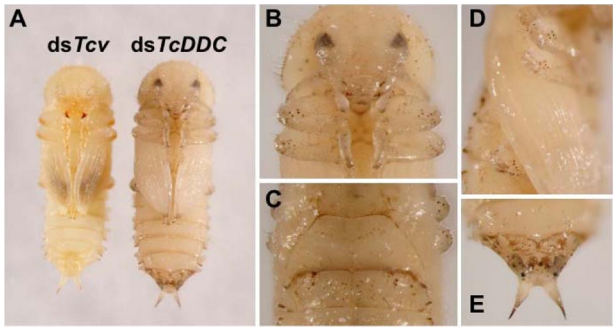

FIGURE 8. **Lethal pupal phenotype produced by injection of dsRNA for *TcDDC* into late larvae.** dsRNA (200 ng per insect) for *TcDDC* was injected into late larvae. The resulting pupal cuticle turned a grayish color and exhibited many minute black patches. The pupa died after 3–5 days. dsRNA for *Tc vermilion* (ds*Tcv*) was injected as a control. *A,* whole body; *B,* head; *C,* dorsal view; *D,* side view; *E,* urogomphi.

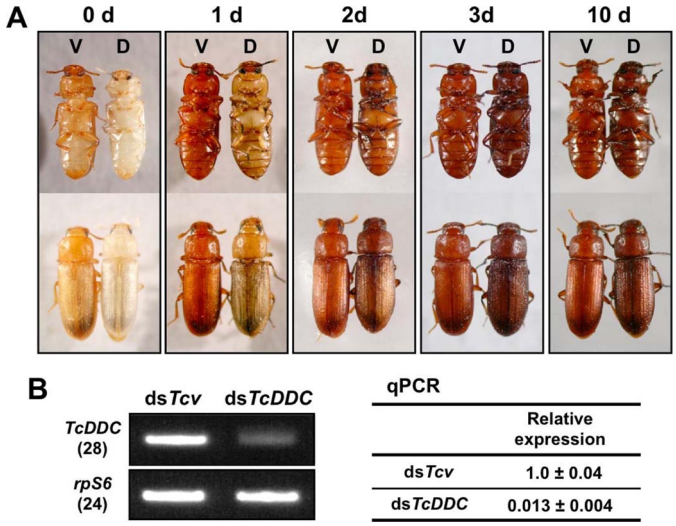

FIGURE 9. **Adult phenotypes produced by injection of dsRNA for *TcDDC*.** *A,* dsRNA (200 ng per insect) for *TcDDC* was injected into 1–2-day-old pupae (*D, right pictures* of each panel). The adult body color turned dark rust-red but not black after injection of ds*DDC*. dsRNA for *vermilion* (ds*Tcv*) was injected as a control (*V, left pictures* of each panel). *B,* knockdown level of *TcDDC* by RNAi. cDNAs for RT-PCR and real time PCR were prepared from total RNA isolated from whole beetles ($n = 3$) at 5 days (3–4-day post-injection). The *numbers* in *parentheses* represent PCR cycles. RT-PCR and real time PCR of *Tribolium* ribosomal protein 6 (*rpS6*) transcript with the same cDNA template served as an internal control. For real time PCR, expression levels of *TcDDC* in ds*TcDDC* treated insects are presented relative to the levels in ds*Tcv* control. *qPCR,* quantitative PCR.

DISCUSSION

Sequence Analysis and Expression of TcADC and TcDDC Transcripts during Development—Enzymes that catalyze the decarboxylation of two amino acids, aspartic acid and DOPA, are hypothesized to participate in insect cuticle tanning metabolism. One, ADC, catalyzes the decarboxylation of aspartic acid to form β-alanine; and the other, DDC, uses DOPA as its substrate to produce dopamine. Dopamine is subsequently *N*-acylated with β-alanine to yield NBAD, one of the major catechols used for cuticle tanning. After searching the *Tribolium* genome data base for *ADC*-like genes, we identified two genes, including an apparent ortholog of the *Drosophila ADC* known as *black* or *Dgad2* (28), which we call *TcADC*, as well as a gene encoding a related protein, G10581. We cloned a full-length *TcADC* cDNA with an open reading frame encoding a protein of 540 amino acid residues. The *Tribolium* genome also encodes an apparent ortholog of *D. melanogaster* glutamate decarboxylase-1 (G09324), as well as another protein (G14177) that groups with the Asp and Glu decarboxylases in a phylogenetic analysis of protein sequences and is very similar to *D. melanogaster* protein CG5618, whose function has not yet been determined. It is conceivable that the proteins in this group, in

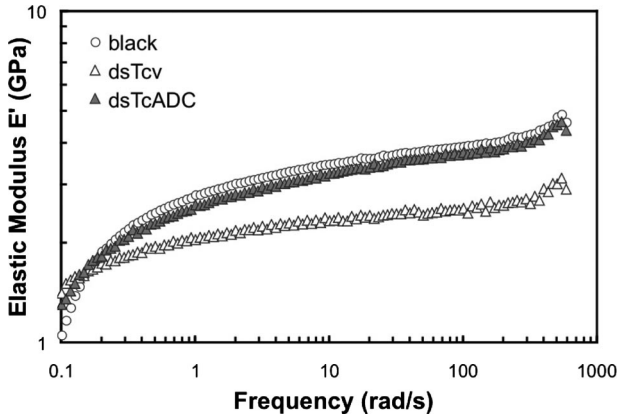

FIGURE 10. **Dependence of the E′ of *Tribolium* elytral cuticle upon frequency of sinusoidally oscillating stress.** Frequency sweeps of a single elytron were performed at 0.2% strain. Each curve is an average of four trials. The lesser frequency dependence displayed by elytra from ds*Tcv*-injected control insects is indicative of a more effectively cross-linked structure than elytra from *black* or ds*TcADC*-injected insects.

TABLE 3

Physical properties of Tribolium elytral cuticle determined by dynamic mechanical analysis

Results are for mature (7–14-day-old) beetle elytra under oscillating stress at 0.2% strain. Each data set is based on four independent tests. The over-under range presented in the table is defined by the 95% confidence interval. GPa is gigapascals.

Sample	E′ at 10 rad/s GPa	n^a	E′/E″ at 10 rad/s
Black	3.5 ± 1.5	0.054 ± 0.008	0.11 ± 0.02
ds*TcADC*	3.2 ± 1.5	0.060 ± 0.009	0.12 ± 0.02
ds*Tcv*	2.3 ± 1.0	0.034 ± 0.004	0.07 ± 0.01

[a] Exponent of power law frequency dependence is E'^n.

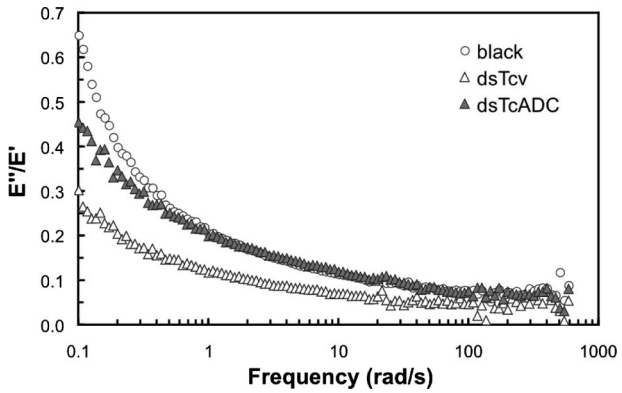

FIGURE 11. **Dependence of the ratio of the E″ to the E′ of *Tribolium* elytral cuticle upon frequency of sinusoidally oscillating stress.** Frequency sweeps of a single elytron were performed at 0.2% strain. Each curve is an average of four trials. Deficiency of ADC is anticipated to reduce cross-linking responsible for the elastic component, and instead to increase melanic pigment production, which would increase the viscous component. The higher E″/E′ ratio observed is consistent with that hypothesis.

addition to TcADC, may have some degree of aspartate decarboxylating activity.

We also identified an apparent ortholog of *D. melanogaster DDC*, which we denoted as *TcDDC*, and we cloned its full-length cDNA. The deduced amino acid sequence (475 amino acids) exhibited high sequence similarity to other insect DDCs as well as to *Drosophila* epidermal DDC. The *DmDDC* gene has two alternatively spliced transcripts, one that is expressed in the epidermis and the other in the central nervous system (15). However, to our knowledge there is no evidence of tissue-specific expression of alternatively spliced *DDC* transcripts in two other species, *Manduca sexta* and *Aedes aegypti* (29, 30). The *Tribolium* genome contains two other genes with high sequence similarity to *TcDDC*, *G13401* and *G13402*. It is feasible that they may also encode proteins with DOPA decarboxylating activity, as may be the case for a related gene in *Drosophila* known as the *α-methyldopa resistance* gene (31, 32).

Developmental expression profiles of *TcADC*, *G10581*, *TcDDC*, *G13401*, and *G13402* were analyzed by RT-PCR, and the transcript levels of *TcADC* and *TcDDC* were further analyzed by real time PCR. The relatively low levels of *TcDDC* transcripts observed during pupal development may be due to some expression in the central nervous system as well as in the epidermis. Transcripts of both *TcADC* and *TcDDC*, however, were dramatically increased at the pharate adult stage (Fig. 3*A*), when *Tribolium* initiates adult cuticle tanning metabolism (Fig. 4*A*, *middle panel*). These data support the hypothesis that TcDDC provides dopamine and TcADC provides β-alanine for subsequent production of NBAD, which serves as a precursor for the quinone-derived cuticle tanning agent, ultimately resulting in the rust-red body coloration of the cuticle of the beetle. The other candidate genes encoding DDC-like proteins (*G13401* and *G13402*) and ADC-like proteins (*G10851*) were expressed little or not at all at the pharate adult stage, suggesting that they lack a major role in providing metabolic precursors for adult cuticle tanning.

Is the Body Color Phenotype of the Tribolium Black Mutant Because of a Mutation in TcADC?—NBAD and NADA are the major catechols in the adult cuticle of the wild-type strain and are associated with the rust-red body color, whereas black pigmentation is associated with lower levels of these catechols and β-alanine, as well as an abnormally high level of dopamine (6) (Fig. 6). ADC and NBAD synthase are key enzymes for producing NBAD from the two precursors dopamine and β-alanine (Fig. 1), and the reduction of β-alanine content in the *black* body color mutant (6) suggested that it might have a mutation in the gene encoding ADC. The *TcADC* gene maps to linkage group LG3 at position 42.6,[3] which is very near the locus of the *black* body color mutant. To analyze whether the *black* mutation occurs in the coding region of the *ADC* gene, we cloned and sequenced a full-length cDNA of *TcADC* from the *black* body color mutant and from the wild-type strain (supplemental Fig. 2). There was no reading frameshift, premature stop codon, or amino acid substitution in the open reading frame encoding the putative catalytic domain (28) of ADC from the *black* mutant. It is quite possible that TcADC in the black body color mutant is enzymatically active but has been down-regulated. We subsequently analyzed the transcript levels of *TcADC* in the *black* mutant as well as in a second black body color mutant strain, b^{Chr}/b^{ST}, and compared them to wild-type levels (Fig. 3*B*). The transcript levels of *TcADC* in these *black* mutant strains were indeed significantly lower than that of the wild-type strain. Real time PCR confirmed that the mRNA level of *TcADC* in the *black* mutant was more than 2 orders of magnitude less than that in wild-type insects, and the transcript was undetectable in the b^{Chr}/b^{ST} strain. These results indicate that the black body

[3] Y. Arakane and R. W. Beeman, unpublished observations.

mutations lead to severely diminished *TcADC* mRNA levels, which limit synthesis of β-alanine used for NBAD production and lead to accumulation of dopamine. Rescue of the black mutant by injection of β-alanine into newly eclosed adults (6) supports this interpretation. The observation that even the b^{Chr}/b^{ST} mutant contained some NBAD (Fig. 6) suggests that alternative decarboxylating enzymes, perhaps those with primary specificity for other substrates such as glutamate, might help to compensate for a lack of TcADC and catalyze the synthesis of some β-alanine from aspartic acid.

Injection of dsRNA for *TcADC* resulted in a black-pigmented adult phenotype similar to that of the *black* mutant strain (Fig. 4*A*). Furthermore, these insects had a nearly 90% reduction in NBAD levels when compared with control insects, together with a higher level of dopamine (Fig. 6). Also β-alanine injection could also rescue the rust-red body pigmentation of the black phenotype produced by injection of dsRNA for *TcADC* (Fig. 5). All of these results support the hypothesis that the *Tribolium black* mutants have a mutation(s) that causes an abnormally low expression of *ADC*. The lack of ADC prevents synthesis of β-alanine used for NBAD production and thus allows for the buildup of abnormally high levels of dopamine, which is used for dopamine eumelanin pigment synthesis (black body coloration) and dopamine quinone-mediated protein cross-linking (Fig. 1). Similarly, knockdown of *TcADC* mRNA in *Tribolium* results in a deficiency of β-alanine and high levels of dopamine, with the latter used instead of NBAD for tanning of the exoskeleton.

Laccase 2 Is Involved in Dopamine/DOPA Eumelanin Pigmentation Pathway—We were interested in determining whether the same or different phenol oxidases influence the cuticle tanning pathway in wild-type and mutant strains of *Tribolium*. Previously, we demonstrated that two isoforms of laccase 2 catalyze beetle cuticle tanning (19). To determine whether TcLac2 also affects these processes in the black body color mutant of *Tribolium*, dsRNA for *TcLac2* was injected into b^{Chr}/b^{ST} late-stage larvae and pharate pupae. dsRNA for *TcLac2* prevented larval, pupal, and adult cuticle tanning of the *black* mutant. The albino phenotypes obtained were similar to those of *TcLac2* RNAi in the wild-type strain of *Tribolium*. In contrast, dsRNA for *TcTyr1*/*Tyr2* had no effect on cuticle tanning in either strain (Fig. 7*B*). This result supports the hypothesis that, in addition to cuticle sclerotization, laccase 2, but not tyrosinase, catalyzes the DOPA/dopamine melanization (pigmentation) pathway in *Tribolium* (Fig. 1).

TcDDC Is Required for Pupal Development—A lethal pupal phenotype was observed after injection of ds*TcDDC* into late-instar larvae (Fig. 8). The pupal cuticle turned a grayish color and exhibited many black-colored patches. This pattern of coloration may be the result of a buildup of high levels of DOPA, some of which are oxidized to DOPA eumelanin in small localized areas only. DOPA cannot serve as a precursor for quinone tanning in most of the pupal cuticle. Huang *et al.* (33) reported some behavioral modifications and high mortality of *Armigeres subalbatus* after silencing of its *DDC* transcript using the double subgenomic Sindbis system, and *DDC* mutants of *Drosophila* have neurological phenotypes (15) because of the role of dopamine as a neurotransmitter. We do not know whether tissue-specific alternative splicing of *TcDDC* mRNA occurs in *Tribolium,* but it is likely that injection of ds*TcDDC* suppressed *TcDDC* transcript levels in the central nervous system also because this tissue is also susceptible to RNAi in *Tribolium*.[3] The lethal pupal phenotype may be due to a down-regulation of transcripts of *TcDDC* in both the epidermis and central nervous system, adversely affecting both pupal cuticle formation and neurotransmission.

DOPA Is a Poor Substrate for Laccase 2—To study the function(s) of *TcDDC* in adult cuticle pigmentation and sclerotization in *Tribolium*, dsRNA for *TcDDC* was injected into 1–2-day-old pupae, and the adults generated were observed. Pupae treated with ds*TcDDC* developed normally. However, the initial adult cuticle pigmentation and sclerotization was substantially delayed (see insects in *0* and *1 d panels i*n Fig. 9). Also, the timing and rate of cuticle tanning of black body-colored beetles were similar to those of wild-type insects, suggesting that dopamine in black body insects is oxidized by laccase 2 and used for dopamine eumelanin synthesis when it accumulated during tanning metabolism. The level of DOPA increased about 5-fold in pharate adults after injection of dsRNA for *TcDDC* into 1–2-day-old pupae. However, unlike dopamine, DOPA does not appear to be well utilized for DOPA eumelanin or DOPA quinone synthesis, perhaps because of the substrate preference of laccase 2. Thomas *et al.* (34) reported that the specific activity of *Manduca* laccase solubilized from pharate pupal integument when DOPA was utilized as the substrate was about 20-fold less than when NBAD was used. Also DOPA is a poor substrate for recombinant *M. sexta* laccase produced using a baculovirus-insect cell line protein expression system.[3] Interestingly, the body color of *TcDDC*-knockdown adults was darker than that of ds*Tcv*-knockdown control beetles, but it was not as dark as any of the *black* body color mutants or *TcADC*-knockdown beetles (Fig. 9). Because DOPA eumelanin and dopamine eumelanin exhibit a similar black pigmentation, this result supports the hypothesis that little DOPA eumelanin accumulates in the *Tribolium* cuticle tanning pathway relative to NBAD- or NADA-mediated pigmentation and dopamine eumelanin, probably because DOPA is a poor substrate for laccase 2.

Mechanical Properties of Elytra from Black Body Color Mutants and dsTcADC-treated T. castaneum—A change in the frequency dependence of the E′ cuticle as well as that of the E″/E′ ratio was observed in response to varying ADC expression. Natural levels of ADC expression present in ds*Tcv*-knockdown control insects imparted the cuticle with an elastic modulus that is relatively frequency-independent, indicating effective cross-linking between cuticular components. In contrast, *black* and ds*TcADC*-treated beetles with reduced ADC levels produced a cuticle that had notably higher frequency dependence. This finding is consistent with the interpretation that a reduced ADC level results in an overabundance of melanin-containing pigments at the expense of cuticular protein cross-linking through NBAD, which requires ADC for production of β-alanine. Our observation that the *black* and ds*TcADC*-knockdown insects have a less cross-linked cuticle is consistent with the hypothesis that the *black* mutant is deficient in *ADC,* which in turn biases the cuticle reaction pathway to

produce a dopamine eumelanin pigment at the expense of NBAD quinone-mediated cross-linking. This conclusion is further supported by the significantly higher E″/E′ ratio found in the ds*TcADC*-injected insects and the black color mutant. The higher ratio suggests a greater dampening ability of such cuticle, consistent with a less cross-linked material. Cuticle from ds*Tcv*-injected control insects exhibited a lower E″/E′ ratio that is less dependent on stress frequency, further suggesting that the wild-type cuticle must possess a greater number of cross-links.

We have shown that tanning of red flour beetle cuticle is regulated in part by the synthesis of β-alanine, dopamine, NBAD, and NADA and also the subsequent oxidation of those catechols by laccase 2. NBAD and NADA are available for production of reddish-brown cuticle, and if β-alanine is unavailable for NBAD synthesis, dopamine, but not DOPA, can be utilized for black cuticle formation. High levels of dopamine in dark body and *TcADC*-knockdown insects occur because of a lack of β-alanine for synthesis of NBAD. *TcDDC* knockdown results in high levels of DOPA and either pupae that cannot tan their cuticles and die or adults with a darker than normal rust red-colored cuticle, which nonetheless still survive.

We have also demonstrated that the mechanical performance of the cuticle can be altered by tampering with the synthesis of specific tanning agents and enzymes using specific dsRNAs or mutants. Specifically, cuticle component cross-linking as indicated by modulus frequency dependence appears to depend on β-alanine and NBAD availability during cuticle formation. This observation further implicates NBAD as an important metabolite for cuticle tanning in *T. castaneum*. Finally, this work also demonstrates the potential of dynamic mechanical analysis to quantify physical differences in phenotype and to help assign a molecular interpretation of these differences. It may be possible to change the mechanical properties of cuticle in desirable ways by changing the ratios of the components needed for cuticle tanning.

Acknowledgment—We thank Jonna Voorhees for beetle husbandry.

REFERENCES

1. Andersen, S. C. (2005) in *Comprehensive Molecular Insect Science* (Gilbert, L. I., Iatrou, K., and Gills, S., eds) Vol. 4, pp. 145–170, Elsevier Press, Oxford, UK
2. Hopkins, T. L., and Kramer, K. J. (1992) *Annu. Rev. Entomol.* **37,** 273–302
3. Kramer, K. J., Kanost, M. R., Hopkins, T. L., Jiang, H., Zhu, Y. C., Xu, R., Kerwin, J. L., and Turecek, F. (2001) *Tetrahedron* **57,** 385–392
4. Hopkins, T. L., Morgan, T. D., and Kramer, K. J. (1984) *Insect Biochem.* **14,** 533–540
5. Morgan, T. D., Hopkins, T. L., Kramer, K. J., Roseland, C. R., Czapla, T. H., Tomer, K. B., and Crow, F. W. (1987) *Insect Biochem.* **17,** 255–263
6. Kramer, K. J., Morgan, T. D., Hopkins, T. L., Roseland, C. R., Aso, Y., Beeman, R. W., and Lookhart, G. L. (1984) *Insect Biochem.* **14,** 293–298
7. Roseland, C. R., Kramer, K. J., and Hopkins, T. L. (1987) *Insect Biochem.* **17,** 21–28
8. Hopkins, T. L., Morgan, T. D., Aso, Y., and Kramer, K. J. (1982) *Science* **217,** 364–366
9. Ujvary, I., Hiruma, K., Riddiford, L. M., Matolcsy, G., Roseland, C. R., and Kramer, K. J. (1987) *Insect Biochem.* **17,** 389–399
10. Andersen, S. O. (2007) *Insect Biochem. Mol. Biol.* **37,** 969–974
11. Haliscak, J. P., and Beeman, R. W. (1983) *J. Econ. Entomol.* **76,** 717–722
12. Beeman, R. W., and Stuart, J. J. (1990) *J. Econ. Entomol.* **83,** 1745–1751
13. Sokoloff, A., Slatis, H. M., and Stanley, J. (1960) *J. Heredity* **51,** 131–135
14. Sokoloff, A. (1977) *The Biology of Tribolium*, Vol. 3, pp. 96–106, Clarendon Press, Oxford, UK
15. Hodgetts, R. B., and O'Keefe, S. L. (2006) *Annu. Rev. Entomol.* **51,** 259–284
16. Arakane, Y., Hogenkamp, D. G., Zhu, Y. C., Kramer, K. J., Specht, C. A., Beeman, R. W., Kanost, M. R., and Muthukrishnan, S. (2004) *Insect Biochem. Mol. Biol.* **34,** 291–304
17. Lorenzen, M. D., Brown, S. J., Denell, R. E., and Beeman, R. W. (2002) *Genetics* **160,** 225–234
18. Arakane, Y., Muthukrishnan, S., Kramer, K. J., Specht, C. A., Tomoyasu, Y., Lorenzen, M. D., Kanost, M., and Beeman, R. W. (2005) *Insect Mol. Biol.* **14,** 453–463
19. Arakane, Y., Muthukrishnan, S., Beeman, R. W., Kanost, M. R., and Kramer, K. J. (2005) *Proc. Natl. Acad. Sci. U. S. A.* **102,** 11337–11342
20. Tomoyasu, Y., and Denell, R. E. (2004) *Dev. Genes Evol.* **214,** 575–578
21. Kumar, S., Tamura, K., and Nei, M. (2004) *Brief. Bioinform.* **5,** 150–163
22. Menard, K. P. (1999) *Dynamic Mechanical Analysis: A Practical Introduction*, p. 84, CRC Press, Boca Raton, FL
23. Ferry, J. D. (1980) *Viscoelastic Properties of Polymers*, 3rd Ed., pp. 33–49, John Wiley & Sons, Inc., New York
24. Koenderink, G. H., Atakhorrami, M., MacKintosh, F. C., and Schmidt, C. F. (2006) *Phys. Rev. Lett.* **96,** 138307
25. Gardel, M. L., Shin, J. H., MacKintosh, F. C., Mahadevan, L., Matsudaira, P. A., and Weitz, D. A. (2004) *Phys. Rev. Lett.* **93,** 188102
26. Hoffman, B. D., Massiera, G., and Crocker, J. C. (2005) arXiv:physics/0504051v2 [physics.bio-ph]
27. Kong, H. J., Wong, E., and Mooney, D. J. (2003) *Macromolecules* **36,** 4582–4588
28. Phillips, A. M., Smart, R., Strauss, R., Brembs, B., and Kelly, L. E. (2005) *Gene* **351,** 131–142
29. Hiruma, K., Carter, M. S., and Riddiford, L. M. (1995) *Dev. Biol.* **169,** 195–209
30. Ferdig, M. T., Li, J., Severson, D. W., and Christensen, B. M. (1996) *Insect Mol. Biol.* **5,** 119–126
31. Marsh, J. L., and Wright, T. R. (1986) *Genetics* **112,** 249–265
32. Black, B. C., Pentz, E. S., and Wright, T. R. (1987) *Mol. Gen. Genet.* **209,** 306–312
33. Huang, C. Y., Chou, S. Y., Bartholomay, L. C., Christensen, B. M., and Chen, C. C. (2005) *Insect Mol. Biol.* **14,** 237–244
34. Thomas, B. R., Yonekura, M., Morgan, T. D., Czapla, T. H., Hopkins, T. L., and Kramer, K. J. (1989) *Insect Biochem.* **19,** 611–622